Investigation of anharmonic lattice vibrations with coherent phonon polaritons

H. J. Bakker, S. Hunsche, and H. Kurz
Institut für Halbleitertechnik II, Rheinisch-Westfälische Technische Hochschule Aachen, D-52056 Aachen, Germany
(Received 17 February 1994)

We investigate the dielectric response of the lowest-energy TO phonon of A_1 symmetry of $LiNbO_3$ via the impulsive excitation and heterodyne detection of THz phonon polaritons. We find that the low-frequency polariton dispersion of $LiNbO_3$ is strongly influenced by four resonances at 1.3, 2.4, 3.4, and 4.1 THz. These resonances lead to avoided crossings in the polariton dispersion and to polariton beats. The presence of these resonances provides strong evidence that the microscopic potential of this phonon is extremely anharmonic and consists of three wells.

I. INTRODUCTION

Lattice vibrations (phonons) are mostly described as a chain of coupled harmonic oscillators.[1] For optical phonons these oscillators are formed by the normal vibrational modes of the ions in the unit cell. In this picture, each optical phonon has a single resonance frequency that depends on the frequency of the normal vibration in the unit cell and the wave vector. However, for ferroelectric crystals it is often observed that there are more optical-phonon resonances than there are normal vibrations in the unit cell.[2–5] The additional resonances are mostly assigned to transitions involving different optical phonons (difference bands, combination bands).[2–4] These transitions become allowed when the phonons are anharmonically coupled. In principle, the observation of additional resonance frequencies can also result from the anharmonic vibrational progression of the individual phonons. For molecules, this type of anharmonicity is a quite common phenomenon, leading to the observation of overtones and frequency-shifted excited-state absorption at elevated temperatures (hot bands).[6] Recently, it was found that the temperature dependence of the asymmetry of the Raman line shape of the lowest-energy A_1 phonon of $PbTiO_3$ could be well explained by this type of anharmonicity.[7]

For many decades, ferroelectric $LiNbO_3$ has been studied because of its enormous merit in nonlinear optics and electro-optics.[8] It has been found that the low-frequency dielectric properties of this crystal are largely determined by the lowest-energy transverse-optical (TO) phonon of A_1 symmetry.[2,3] This phonon has a resonance frequency of 7.5 THz at 300 K and is often referred to as the ferroelectric mode because it plays an important role in the ferroelectric phase transition.

The frequency spectrum of phonons is usually investigated with Raman scattering and infrared spectroscopy. Unfortunately, these techniques suffer from bad signal-to-noise ratios at low frequencies (<5 THz). Recently, it has been shown that the low-frequency dielectric response can also be investigated with phonon polaritons that are impulsively excited by ultrashort laser pulses.[9–14] Phonon polaritons are mixed light-polarization states that arise from the coupling of far-infrared light with phonon resonances. The coupling of the light with a resonance leads to the formation of two polariton-dispersion branches that have an avoided crossing.[1] Recent experimental investigations showed that the study of the dispersion and damping of phonon polaritons provides valuable information on the frequencies, the absorption strengths, and the widths of the phonon resonances.[9–14]

In this paper we report on the investigation of the dielectric response of $LiNbO_3$ by the impulsive excitation and heterodyne detection of phonon polaritons with ultrashort laser pulses. The measured phonon-polariton dispersion at 300 K shows the presence of four low-frequency resonances. We will show that this observation can be explained from the extreme anharmonicity of the lowest-energy TO phonon of A_1 symmetry of $LiNbO_3$.

II. EXPERIMENTAL DETAILS

The phonon polaritons are excited and probed using laser pulses with a pulse duration of 60 fs, a central wavelength of 625 nm, and an energy per pulse of 5 μJ. These laser pulses are split into three. Two of the three pulses serve as excitation pulses and are focused into the sample under a chosen angle to a common focus with a diameter of 200 μm. These pulses enter the crystal simultaneously and generate THz phonon polaritons by difference-frequency mixing and stimulated Raman scattering. This excitation process leads to the generation of two counterpropagating phonon polaritons of equal frequency and amplitude. The pump beams are polarized along the optical axis in order to attain the highest excitation efficiency. The generated polaritons are also polarized along this axis. The wave vector of the polaritons is determined by the difference of the wave vectors of the two pump beams and can be tuned by varying the angle between these beams. The polariton frequency that corresponds with this wave vector is selected out of the broad bandwidth of the laser pulses.

0163-1829/94/50(2)/914(7)/$06.00

The polaritons are phase-sensitively detected with a time-delayed third pulse (probe). The periodic electric field of the polaritons will modulate the refractive index as a result of the electro-optic effect. The resulting index grating will diffract the probe pulse. The probe is polarized along the optical axis to optimize the electro-optic effect. The frequency and damping of the polaritons are determined by measuring the diffracted-light intensity as a function of the delay between the probe and the two excitation pulses. When the probe is focused at the same spot as the two excitation pulses, the diffracted light will be modulated with the double polariton frequency due to the interference of the two generated counterpropagating polaritons.[11,14] This technique only allows a correct determination of the polariton frequency if the frequency spectrum of the polariton peaks at only one frequency. However, if the frequency spectrum of the polaritons consists of two or more overlapping peaks, the light diffracted by two counterpropagating polaritons will not be modulated with the double frequency of each maximum but rather with their *sum* frequency.[13] Then, it is no longer possible to determine the different maxima of the frequency spectrum of the polaritons from the diffracted signal. To avoid this problem, we use a different method for the determination of the polariton frequency. In our experiment, the probe pulse focus is shifted with respect to the common focus of the excitation pulses. As a result, only one of the two polaritons will propagate into overlap with the probe after a certain delay. In this case, the amplitude of the diffracted electric field will not be periodically modulated and in principle only the envelope of the polariton will be observed. However, the phase of the diffracted electric field changes continuously with the polariton frequency. By letting the diffracted electric field interfere with probe light with a delay-independent phase, the signal in the diffracted direction will get modulated with the single polariton frequency. The probe light with delay-independent phase is obtained from scattering from imperfections at the surface of the crystal. This heterodyne detection technique allows a direct and accurate determination of the polariton frequency spectrum, even if this spectrum consists of several peaks.

In our experiment, we will mainly observe polaritons with strong light character because of two effects. In the first place, due to the large $\chi^{(2)}$ of $LiNbO_3$, the polaritons are predominantly excited over their light character via difference-frequency mixing. As a result, lightlike polaritons will be excited with a much larger amplitude than phononlike polaritons. Second, in our experiment the polaritons have to propagate a few hundred micrometers before they can be detected by the probe pulse. Only lightlike polaritons will still have a significant amplitude after this propagation length because they are weakly damped and have a large group velocity. The phononlike polaritons are strongly damped and hardly propagate so that they will never reach the probe spot. As a consequence, in our experiment the lower branch of the polariton dispersion will be observed at low wave vectors and the upper branch at high wave vectors. However, near an avoided crossing, the two polariton branches have about equal light character so that both can be observed.

III. RESULTS AND DISCUSSION

In Fig. 1 six time-resolved measurements of polaritons are presented after background substraction. We find that at most wave vectors the time-resolved signal is formed by a regular oscillation which implies that at these wave vectors a single polariton frequency is generated. However, for wave vectors near 1500, 3000, and 4000 cm^{-1}, strong beating phenomena (polariton beats) are observed. The Fourier transform of these measurements show that at these wave vectors two or even three [Fig. 1(d)] different polariton frequencies are coherently excited. This observation of several polariton frequencies at one wave vector forms a strong indication for the presence of low-frequency resonances that lead to avoided crossings in the polariton dispersion. We find four avoided crossings in the low-frequency polariton dispersion of $LiNbO_3$ indicative of four weak resonances at 1.3, 2.4, 3.4, and 4.1 THz (Fig. 2). The frequency gap of each avoided crossing is determined by the absorption strength of the resonance. The avoided crossings associated with the resonances at 3.4 and 4.1 THz are close so that for wave vectors near 3500 cm^{-1} there exist three polariton dispersion branches with strong light character. As a consequence, three different polariton frequencies can be observed simultaneously [Fig. 1(d)].

The low-frequency resonances were not observed in a previous time-resolved study on phonon polaritons in $LiNbO_3$.[11] However, in this latter study the polariton frequencies were not determined with a heterodyne detection technique but were derived from the modulation of the diffracted light that results from the interference of the two generated counterpropagating polaritons. In a previous Raman-scattering study on $LiNbO_3$ a weak signal was observed between 2.5 and 4 THz,[4] but the signal was too weak to determine the resonance frequencies.

The four resonances cannot be assigned to transitions between different normal lattice vibrations, because the observed frequencies do not fit the energy differences of the optical phonons of $LiNbO_3$. In addition, the observed absorption strengths of these resonances can only be explained from difference bands if the anharmonic couplings are extremely strong. Hence, it seems to be much more likely that the four resonances result from the anharmonicity of the phonon *itself*. It has been shown previously that this type of anharmonicity can have a strong effect on the Raman spectrum of low-energy lattice vibrations.[7] In addition, the important role of the lowest-energy TO phonon of A_1 symmetry in the ferroelectric phase transition is a strong indication that the microscopic potential of this phonon is strongly anharmonic.[15]

The measured polariton dispersion can be used to determine the shape of the microscopic potential of the phonon. The polariton dispersion is given by the maxima of the polariton response,[16]

$$R(k_p,\omega_p) = \mathrm{Im}\left\{\frac{1}{(c^2k_p^2/\omega_p^2) - \epsilon(\omega_p)}\right\}, \qquad (3.1)$$

with c the velocity of light in vacuum, $\epsilon(\omega)$ the dielectric

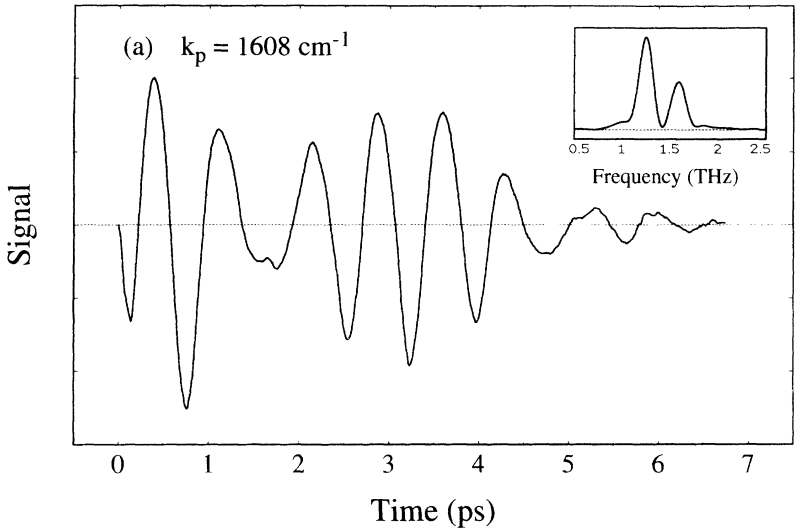

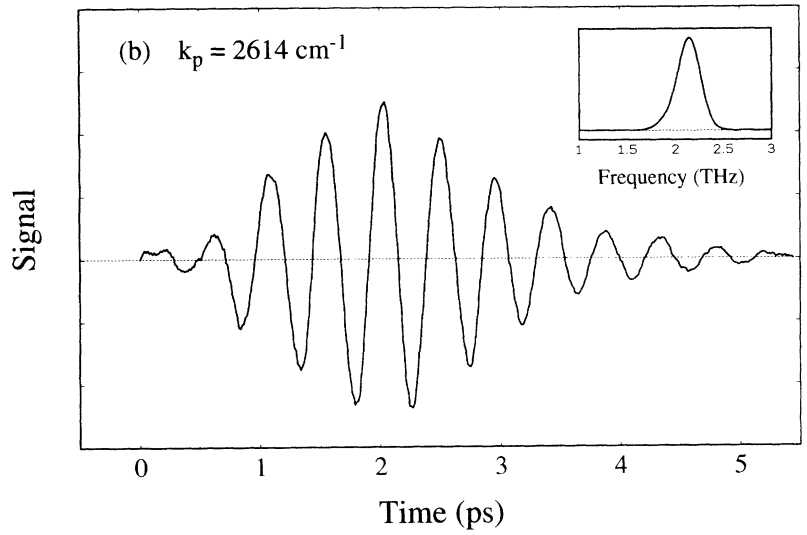

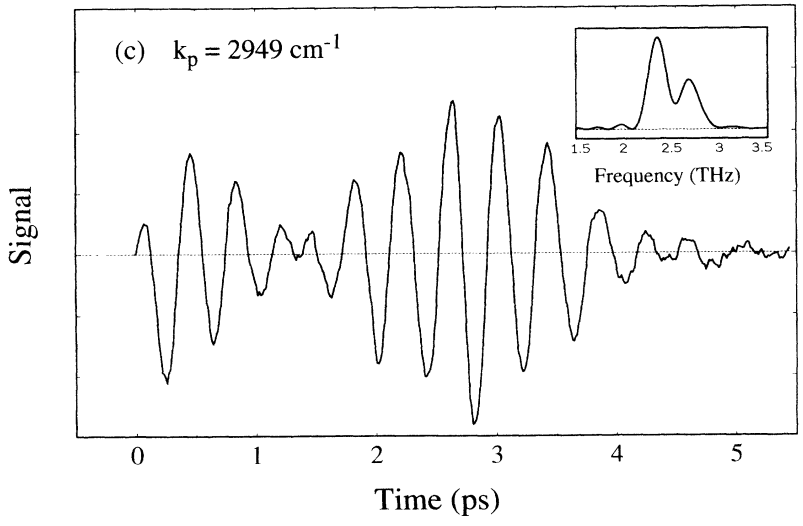

FIG. 1. Time-resolved measurements of phonon polaritons in $LiNbO_3$ at six different wave vectors. The signal is presented as a function of the delay between the two pump pulses and the probe. The background has been substracted. In the inset the Fourier transform of the time-resolved measurements is shown.

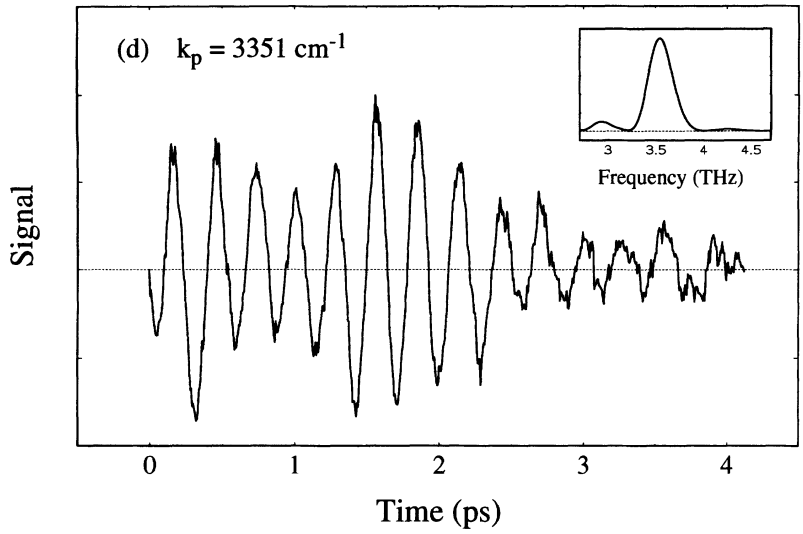

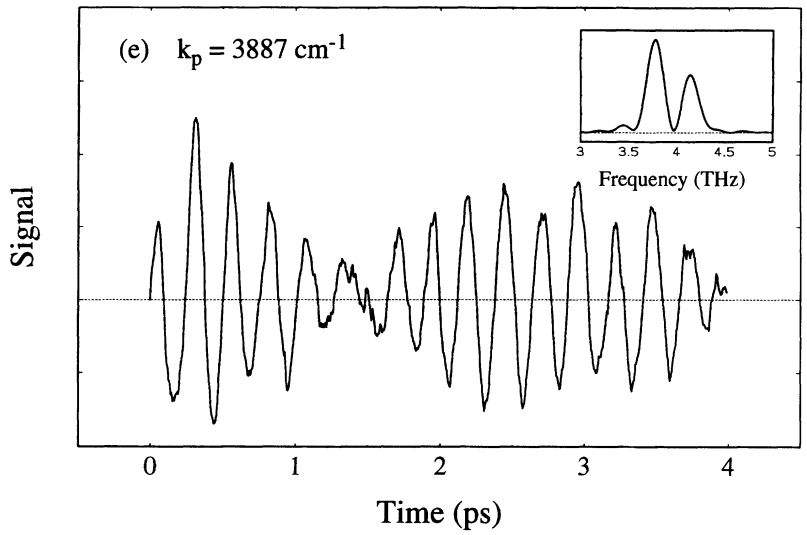

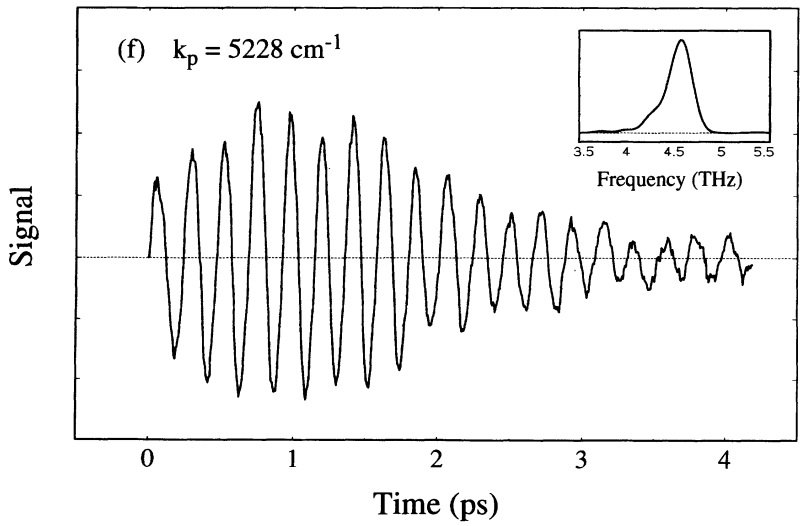

FIG. 1 *(Continued).*

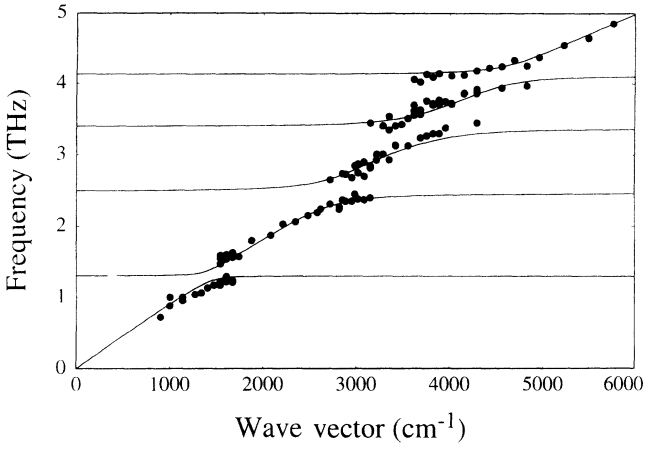

FIG. 2. Phonon-polariton dispersion of $LiNbO_3$ at 300 K. The measurements are represented by points. The solid curves are calculated from the transitions between the vibrational levels in the potential for the ferroelectric mode that is presented in Fig. 3.

function, ω_p the angular frequency of the polariton, and k_p the wave vector of the polariton.

The polariton dispersion measured in our experiment depends on the low-frequency dielectric function for electric fields along the optical axis. In principle, this dielectric function can be calculated by taking into account all possible transitions between vibrational levels in the microscopic potential. However, this potential is strongly influenced by the local electric field that results from the spontaneous polarization of the crystal. For temperatures near the ferroelectric phase-transition temperature, this local field will significantly contribute to the dielectric response.[13] For the present experiments, this contribution can be neglected since the temperature of 300 K is well below the phase-transition temperature of 1480 K. Hence, we only consider the contribution of the transitions between the vibrational levels in the potential:

$$\epsilon(\omega_p) = \sum_{i,j} \frac{2(N_i - N_j)e^2|\mu_{ij}|^2\omega_{ij}/(\epsilon_0\hbar)}{\omega_{ij}^2 - \omega_p^2 - 2i\omega_p/T_{2,ij}}. \tag{3.2}$$

In this equation the indices i and j denote two vibrational levels, N_i and N_j are the populations of these levels, μ_{ij} is the transition dipole moment, $\hbar\omega_{ij}$ is the energy difference, and $T_{2,ij}$ is the damping time constant of the transition between levels i and j. The population of the levels is given by a Boltzmann distribution.

The observation that the frequencies of the four resonances are much lower than 7.5 THz indicates that the microscopic potential consists of a narrow region in which the energy spacing of the vibrational levels is about 7.5 THz and a wider region in which the energy spacing is much smaller. Hence, it seems likely that the potential consists of two or more wells separated by barriers. Figure 3 shows the lower part of the potential that produces the best fit to the measured polariton dispersion and the mean displacement of the Li^+ ion at 300 K (0.051 nm). This potential contains three wells of which two are shown and is presented as a function of the displacement of the Li^+ ion. This displacement is linearly proportional to the normal-mode coordinate r. The dimension of r is length times square root of mass. The two outer wells of the potential are described with a Morse potential and the central well with a harmonic potential. The wells are interconnected by a cubic spline. The following equation gives the potential energy in atomic units as a function of r in atomic units:

$$V(r) = \begin{cases} 0.19(e^{-2.024\times10^{-3}(r-221.9)} - 1)^2 + 2.665\times10^{-2}\langle r\rangle r & \text{if } |r| > 194 \text{ a.u.}, \\ 2.81\times10^{-7}r^2 + 2.665\times10^{-2}\langle r\rangle r & \text{if } |r| < 66 \text{ a.u.} \end{cases} \tag{3.3}$$

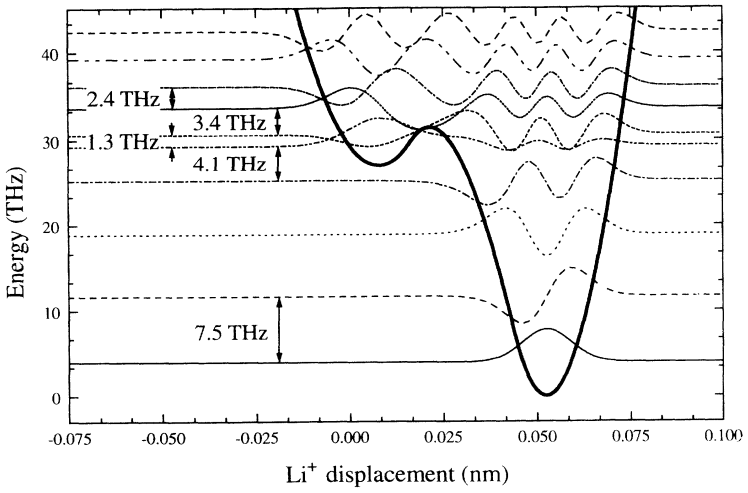

FIG. 3. Potential-energy curve and the ten lowest-energy vibrational wave functions for the ferroelectric mode of $LiNbO_3$ as a function of the displacement of the Li^+ ion along the optical axis. This potential provides the best fit of the measured polariton dispersion shown in Fig. 2.

The local field is proportional to the mean displacement $\langle r \rangle$. The contribution of the local field to the potential energy is respresented by the term proportional to $\langle r \rangle r$.

The frequencies and absorption strengths of the transitions are very sensitive to the shape of the potential. The absolute absorption strength of the resonances is obtained by scaling the calculated transition-dipole moments of the 7.5 THz transitions to the previously measured contribution of this resonance to the static dielectric constant.[3] The calculated absorption strengths and contributions to the static dielectric constant of the resonances at 1.3, 2.4, 3.4, 4.1, and 7.5 THz are presented in Table I. The low-frequency dielectric function of $LiNbO_3$ is calculated using Eq. (3.2). In this calculation we consider all possible vibrational transitions involving the lowest 20 vibrational levels in the potential of Fig. 3. We assume a T_2 of 1 ps for the transitions that lead to the resonances at 1.3, 2.4, 3.4, and 4.1 THz and a T_2 of 500 fs for the transitions that contribute to the resonance at 7.5 THz. The resulting dielectric function is presented in Fig. 4. This dielectric function agrees quite well with the results obtained in previous infrared-reflectivity measurements,[3,17] except of course for the low-frequency resonances that were not detected in the previous measurements.

The dielectric function allows a direct determination of the polariton dispersion using Eq. (3.1). The calculated polariton dispersion is represented by the solid curves in Fig. 2. We find that the frequencies and the frequency gaps of the avoided crossings in the measured polariton dispersion are well reproduced by the results of the calculation. We find that it is not possible to fit the measured polariton dispersion and the displacement of the ions using a single- or double-well potential. For these potentials, a correct fit of the displacement of the ions at 300 K would lead to too low transition frequencies and vice versa. Hence, the observed resonance frequencies form strong evidence for the presence of three wells in the potential of the lowest-energy TO phonon of A_1 symmetry of $LiNbO_3$. The present finding of three wells in the potential does not agree with a previous theoretical study in which it was found that the temperature dependence of the mean displacement of the ions and the static dielectric constant could be described best with an anharmonic single-well potential.[15] However, these macroscopic parameters result from the combined effect of all resonances and are thus not very sensitive for the energy differences between high-energy levels in the potential. Indeed it was shown for $LiTaO_3$ that these macrosopic parameters can be fitted with strongly different microscopic potentials.[18]

TABLE I. Absorption strengths and contributions to the static dielectric constant of the resonances of the lowest-energy A_1 TO phonon of $LiNbO_3$ at 300 K.

Transition	Frequency	$Ne^2\lvert\mu\rvert^2$	ϵ_{st}
$v=0\rightarrow 1$, $v=1\rightarrow 2$, $v=2\rightarrow 3$	7.5 THz	560×10^{-34} C^2 m^{-1}	16.00
$v=3\rightarrow 4$	4.1 THz	4.8×10^{-34} C^2 m^{-1}	0.25
$v=4\rightarrow 5$	1.3 T Hz	6.8×10^{-34} C^2 m^{-1}	1.13
$v=5\rightarrow 6$	3.4 THz	12.5×10^{-34} C^2 m^{-1}	0.79
$v=6\rightarrow 7$	2.4 THz	15.9×10^{-34} C^2 m^{-1}	1.42

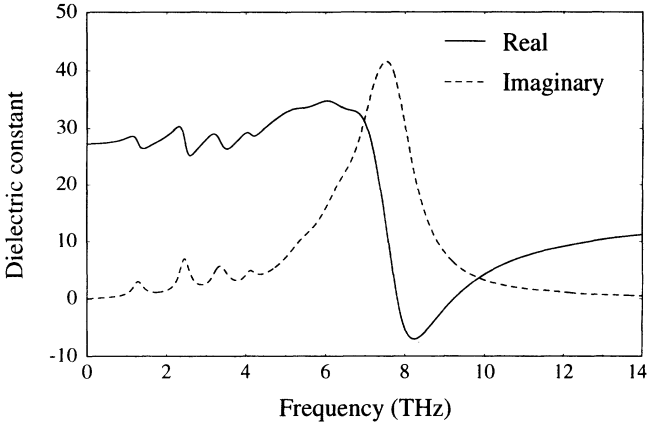

FIG. 4. Low-frequency dielectric function of $LiNbO_3$. The dielectric function is calculated using Eq. (3.2), considering all possible transitions between the 20 lowest vibrational levels in the potential of Fig. 3.

Figure 3 shows that the strong resonance at 7.5 THz can be assigned to transitions between vibrational levels that are localized in the lowest well. The dielectric response strongly depends on the energy difference between the minima of the lowest and the middle well. If the lowest well would be deeper and would contain one additional vibrational level, the resonance at 7.5 THz would be far too strong compared to the other resonances. The low-frequency resonances can all be assigned to transitions between vibrational levels that are delocalized over the lowest and the middle well. The resonances at 1.3 and 4.1 THz are due to transitions between levels with vibrational energies below the top of the barrier. Hence these resonances are tunneling resonances and are associated with the classically forbidden oscillation of the Li^+ ion between the lowest and the middle well. The transition-dipole moments and thus the absorption strengths of the resonances at 1.3 and 4.1 THz are relatively small because these transitions take place between two levels of which one is predominantly localized in the lowest well, while the other is predominantly localized in the middle well. The absorption strengths of the resonances at 2.4 and 3.4 THz are larger, because these resonances result from transitions between vibrational levels that are delocalized over both wells. As a result, the energy gaps of the avoided crossings at 2.4 and 3.4 THz in the polariton dispersion are larger than the energy gaps of the avoided crossings at 1.3 and 4.1 THz. The transitions between higher-energy vibrational levels in the potential all have frequencies near 3.4 THz and thus contribute to the absorption strength of the resonance at this frequency. However, the occupation of these levels is so small that they have little effect on the polariton dispersion.

The presented results show that the anharmonicity of the phonon itself can be that important that many

resonance frequencies are observed for a single optical phonon. Hence, the observation of more resonance frequencies than there are optical phonons may very well result from this type of anharmonicity and is not necessarily the result of transitions involving different optical phonons.[2–4]

IV. CONCLUSIONS

We showed that the low-frequency dielectric response of $LiNbO_3$ can be investigated in detail by the impulsive excitation and heterodyne detection of phonon polaritons. We find that this response is influenced by four resonances at 1.3, 2.4, 3.4, and 4.1 THz. These resonances lead to avoided crossings in the polariton dispersion and to the observation of phonon-polariton beats. The presence of these resonances provides direct evidence that the microscopic potential of the lowest-energy TO phonon of A_1 symmetry is extremely anharmonic and consists of three wells. The measured polariton dispersion allows an accurate determination of the shape of the barriers and the wells of the potential. These results demonstrate that the impulsive excitation and time-resolved heterodyne detection of phonon polaritons form a powerful technique to investigate the anharmonicity of lattice vibrations.

ACKNOWLEDGMENTS

The research presented in this paper is partly supported by the Deutsche Forschungsgemeinschaft and the A. v. Krupp Foundation.

[1] G. Burns, *Solid State Physics* (Academic, Orlando, 1985).
[2] W. D. Johnston, Jr. and I. P. Kaminov, Phys. Rev. **168**, 1045 (1968).
[3] A. S. Barker, Jr. and R. Loudon, Phys. Rev. **158**, 433 (1967).
[4] R. Claus, G. Borstel, E. Wiesendanger, and L. Steffan, Z. Naturforsch. A **27**, 1187 (1972).
[5] A. F. Penna, A. Chaves, P. da R. Andrade, and S. P. S. Porto, Phys. Rev. B **13**, 4907 (1976).
[6] G. Herzberg, *Molecular Spectra and Molecular Structure I: Spectra of Diatomic Molecules* (D. van Nostrand, Princeton, 1965).
[7] C. M. Foster, Z. Li, M. Grimsditch, S.-K. Chan, and D. J. Lam, Phys. Rev. B **48**, 10160 (1993).
[8] S. C. Abrahams *et al.*, *Properties of $LiNbO_3$*, EMIS Datareviews No. 5 (Inspec, London, 1989).
[9] K. P. Cheung and D. H. Auston, Phys. Rev. Lett. **55**, 2152 (1985); D. H. Auston and M. C. Nuss, IEEE J. Quantum Electron. **QE-24**, 184 (1988).
[10] J. Etchepare, G. Grillon, A. Antonetti, J. C. Loulergue, M. D. Fontana, and G. E. Kugel, Phys. Rev. B **41**, 12362 (1990).
[11] P. C. M. Planken, L. D. Noordam, J. T. M. Kennis, and A. Lagendijk, Phys. Rev. B **45**, 7106 (1991).
[12] T. P. Dougherty, G. P. Wiederrecht, and K. A. Nelson, J. Opt. Soc. Am. B **9**, 2179 (1992); T. P. Dougherty, G. P. Wiederrecht, K. A. Nelson, M. H. Garret, H. P. Jensen, and C. Ward, Science **258**, 770 (1992).
[13] H. J. Bakker, S. Hunsche, and H. Kurz, Phys. Rev. Lett. **69**, 2823 (1992); Phys. Rev. B **48**, 13524 (1993).
[14] D. P. Kien, J. C. Loulergue, and J. Etchepare, Opt. Commun. **101**, 53 (1993).
[15] M. E. Lines, Phys. Rev. B **2**, 698 (1970).
[16] A. S. Barker, Jr. and R. Loudon, Rev. Mod. Phys. **44**, 18 (1972).
[17] J. L. Servoin and F. Gervais, Solid State Commun. **31**, 387 (1979).
[18] M. E. Lines, Solid State Commun. **10**, 793 (1972).